Temperature-dependent relaxation and growth phenomena in strained $In_xGa_{1-x}As$ layers grown on GaAs

M. J. Ekenstedt, T. G. Andersson, and S. M. Wang
Department of Physics, Chalmers University of Technology and University of Göteborg, S-412 96 Göteborg, Sweden
(Received 16 November 1992; revised manuscript received 14 April 1993)

A series of $In_xGa_{1-x}As/GaAs$ layers with x ranging from 0.36 to 1 was grown by molecular-beam epitaxy, in order to examine the dependence of the critical layer thickness (CLT) on the In mole-fraction and growth temperature. Reflection high-energy electron diffraction (RHEED) and photoluminescence (PL) measurements were used and indicated a reduced CLT with increasing substrate temperature. A large difference in CLT was found between layers examined by RHEED and PL. This is discussed and explained to be a consequence of the difference in layer structure between layers examined by PL and by RHEED. While RHEED is a surface sensitive method, the luminescence in PL experiments originates from embedded layers. In PL measurements the thickness of the onset of three-dimensional growth, t_{3D}, decreased from 55 to 15 Å for $In_{0.36}Ga_{0.64}As$ layers as the growth temperature increased from 470 to 570 °C. The PL study also indicated a reduced temperature dependence with increasing In content. The RHEED measurements for $In_{0.36}Ga_{0.64}As$ showed that the thickness when the surface lattice parameter becomes equal to that of the alloys varied from 95 to 10 Å for growth temperatures between 490 and 590 °C, respectively. Calculations by the most frequently used models for estimating the CLT were also carried out. The model of Price [Phys. Rev. Lett. **66**, 469 (1991)] best fits our experimental results. The carrier mobility in 2-μm-thick InAs layers was measured between 20 and 300 K for layers grown at substrate temperatures between 390 and 525 °C. The results indicate a peak mobility of 17 266 $cm^2/V\,s$ at 300 K for a structure grown at 520 °C and a peak mobility at 77 K of 34 000 $cm^2/V\,s$ for a sample grown at 510 °C.

I. INTRODUCTION

The knowledge of strained semiconductor layers is very important, since these are part of many electronic and photonic device structures. The full potential of such devices will not be reached unless growth phenomena taking part in strained layer epitaxy and structural restrictions induced by strain are fully understood. Because of the 7% mismatch between the lattice constants in GaAs and InAs, structural defects will occur at a critical layer thickness (CLT) when $In_xGa_{1-x}As$ is grown on GaAs. Defects, which deteriorate the crystal quality, are dislocations, stacking faults, and three-dimensional (3D) islands. The control of growth is further complicated by the tendency of In to segregate at the growth surface. This will to a certain extent reduce the intended In concentration in the layers.

Several experimental techniques have been used in previous studies of CLT. These include photoluminescence (PL),[1–7] x-ray double-crystal diffraction,[5,8–10] Hall effect,[1,4] transmission electron microscopy (TEM),[6,10–12] cathodoluminescence (CL),[10] and reflection high-energy electron diffraction (RHEED).[13–17] The reported values of CLT exhibit large variations due to different thickness resolution in experiments, variations in the criteria used to define CLT, and differences in data analysis. The most common models to predict CLT are the mechanical equilibrium models by Matthews and Blakeslee [18,19] (MB) and Tsao and Dodson (TD),[21] the energy balance models by People and Bean[20] (PB) and Marée *et al.*[11] and, finally, the plastic flow model by Dodson and Tsao (DT),[22,23] which describes the time-delayed relaxation in strained structures. Among them, the MB is the most widely exploited, while the others have been used to fit a few experimental results.[8,9,11,16] More recent investigations[24–29] of $In_xGa_{1-x}As$ growth on GaAs have focused on the In sticking coefficient and revealed its dependence on both substrate temperature and strain.

This paper concerns CLT of the $In_xGa_{1-x}As/GaAs$ system and its relation to molecular-beam-epitaxy (MBE) growth parameters. Such knowledge is important for the growth of high-quality device material, especially highly strained layers. We have used PL and RHEED to study variations with both indium content and growth temperature. The ability to relate the distance between diffraction rods in RHEED patterns to the surface periodicity enabled us to measure the change in lattice parameter with the thickness of an $In_{0.36}Ga_{0.64}As$ layer. The results showed that the surface layer attained the $In_{0.36}Ga_{0.64}As$ lattice parameter as the layer thickness reached 10 Å for layers grown at 590 °C. The corresponding value for growth at 490 °C was much larger, 95 Å. A comparison between the models was carried out and discussed. To fit our RHEED results and to estimate the activation energy for dislocation glide in $In_{0.36}Ga_{0.64}As/GaAs$ structures, the model by Dodson and Tsao[22,23] (DT) was used. Embedded alloy layers with $x = 0.36$, 0.5, 0.8, and 1 were studied by PL. For these high In concentrations, CLT was defined as the onset of three-dimensional (3D) growth t_{3D}. This was found to vary with both In content and growth temperature and was for the first time analyzed for structures with an In mole fraction larger than 0.36. No PL emission was detected for $In_{0.36}Ga_{0.64}As$ layers grown below 470 °C.

To investigate if this was related to a higher incorporation of impurities at low growth temperatures, carrier concentration and mobility were measured by the Hall effect. The highest mobility at 300 K was $\sim 17\,200$ $cm^2V\,s$ for a 2-μm-thick InAs film grown at 520 °C while it dropped to $\sim 11\,000$ $cm^2/V\,s$ for a film grown at 410 °C.

Our work, in part, confirms earlier findings from RHEED investigations[15–17] of surface roughening through 3D growth and measurements of the lattice constant as a function of layer thickness. We also compare CLT in surface layers and embedded structures. In addition, we introduce a more complete description of CLT, where it is defined either as the thickness where the lattice relax through misfit dislocations or the thickness where 3D growth occurs. Experimental results obtained from the comparison between PL and RHEED measurements indicated large differences between CLT in embedded and surface layers.

The paper is organized in the following way. In Sec. II the experimental details are described. The results in Sec. III show a declining CLT with increasing growth temperature. Section IV includes a discussion of the data collected from RHEED, PL, and mobility measurements, and the conclusions are presented in Sec. V.

II. EXPERIMENT

The structures were grown, using solid source techniques, on In-mounted (100) semi-insulating GaAs substrates in a modified Varian MBE-360 system, consisting of a growth chamber, a buffer chamber, and a load-lock system. A cracker for the arsenic source provided dimers resulting in a lower arsenic background when compared to the use of As_4. The vacuum during growth was typically 5×10^{-8} torr. Indium, Ga, and As_2 fluxes were controlled using a beam gauge placed in the substrate position. The group-III/V partial saturation pressure was typically 1/15. RHEED oscillations were used to calibrate the growth rate. As in all MBE systems equipped with a rotating substrate holder, a correct reading of the substrate temperature is difficult to accomplish, since the substrate thermocouple is not in direct contact with the substrate. Normally, this is solved by using a pyrometer for temperatures above 500 °C. For lower temperatures the pyrometer reading is uncertain. For this reason we developed a temperature probe[30,31] working in a nongrowth position capable of giving correct temperature measurements from 375 to 530 °C with a reproducibility of ± 2 °C.

All layers were deposited onto a 0.5–1-μm-thick buffer layer. The structures, grown at 470–590 °C contained a series of $In_xGa_{1-x}As$ quantum wells (QW's) separated by 500–2000-Å-thick GaAs layers. According to our previous TEM results,[32] a 200-Å-thick separation layer is enough to prevent strain (i.e., visible contrast) from the embedded $In_{0.36}Ga_{0.64}As$ layers to mediate through the GaAs layers into subsequential alloy layers. All QW's for the PL measurements were grown without interruption, except for InAs where a 5-s interruption was used prior to and after deposition.

The PL measurements were performed at 77 K with a He-Ne laser as the excitation source. Emission was dispersed by a 1-m SPEX 1704 monochromator and detected by an S-1 photomultiplier together with a conventional lock-in amplifier. To precisely assign each PL peak to its corresponding QW, the structure was etched using a solution of H_2SO_4:H_2O_2:H_2O(1:8:80) giving an etching rate of 0.6 μm/min. Finally, the exact etching depth was determined by a surface profiler.

The RHEED pattern was recorded *in situ* by a standard VHS camera. After growth the videotape was analyzed in a Teragon 4000 image-processing system. Here, the changes in the diffraction pattern and lattice parameter were measured as a function of increasing film thickness. The limited signal-to-noise over from the RHEED screen restrained the resolution of the lattice parameter to an estimated ± 0.05 Å. This was sufficient since most of the interesting information was contained in the trend when the lattice parameter changed from that of GaAs to $In_{0.36}Ga_{0.64}As$.

The Hall samples consisted of a 2-μm-thick undoped InAs film, grown at 390 °C to 525 °C under $(2X4)$ reconstruction on top of a 1-μm-thick GaAs buffer layer. After growth the substrate was etched in HCl to remove the indium mounting. A thin layer of wax protected the surface of the substrate during etching and was later removed by trichloroethylene. The mobility was measured between 20 and 300 K by the Hall effect using the Van der Pauw method. Metal contacts on square samples (3×3 mm^2) were made by In dots which become Ohmic without annealing.

III. RESULTS

A. Photoluminescence measurements

In Fig. 1 typical PL spectra are shown for a sample grown at 490 °C with In content $x=0.8$ and nominal QW thickness $L_z=2$, 3, 4, and 5 monolayers (ML's). Emission at 1296.7 and 1367.5 meV, in curve (a), is attributed to excitonic recombination from the 5- and 4-ML QW's, respectively, the full width at half maximum (FWHM) of both peaks are rather large, approximately 50 and 38 meV. A small tail is observed at the high-energy side of the 4-ML peak. This is clearly shown in curves (b) and (c), where a peak developed after the 5-ML-thick QW was removed. For these measurements excitation intensities of 5 and 10 W/cm^2 were used. The weak emission from the 3 ML's at 1460.5 meV, increased in intensity after etching away the 5-ML QW. The peak size became even more pronounced when the structure was exposed to a higher excitation intensity, curve (c). The peak energy of the 4-ML QW was slightly blueshifted, 5.6 meV, after etching away the thickest QW. It can also be seen that the emission from the 3-ML QW was redshifted by approximately 10 meV. The very weak emission from the 2-ML-thick QW shown in curve (d) could only be observed when the three upper QW's had been removed. Since the 2- and 3-ML wells gave peaks with low FWHM, 7.3 and 11.3 meV, respectively, these layers have a 2D characteristic. The FWHM's from InAs

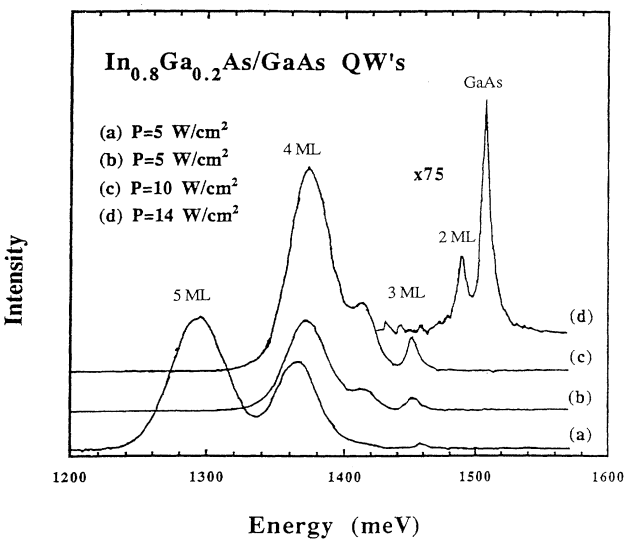

FIG. 1. Photoluminescence spectra for $In_xGa_{1-x}As/GaAs$ QW's grown at 490 °C with nominal layer thickness $L=2$, 3, 4, and 5 ML's. Spectra (b) and (c) were recorded at different excitation intensities after the top QW (5 ML) was removed by etching. In spectrum (d) all QW's except the 2-ML structure were removed.

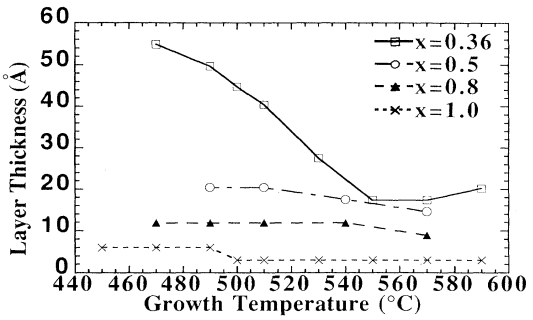

FIG. 2. The onset of three-dimensional growth from PL measurements, t_{3D}^P as a function of growth temperature for x ranging between 0.36 and 1. For $x=0.36$ there is a strong dependence on temperature. The slight increase in t_{3D}^P above 570 °C reflects the decreased sticking coefficient of In at high temperatures. As x increases the influence from the growth temperature on the t_{3D}^P is decreasing.

(QW)'s with nominal thickness of 1 and 2 ML's (not shown here) were about 7 meV. This narrow FWHM is a result of smooth interfaces arising from growth interruption. The illumination spot on the samples was varied, before etching the sample, to measure sample uniformity. Both the FWHM and the peak position showed small variations. Intensity variations among the PL spectra depended on differences in excitation intensities and sample thicknesses (due to etching). The spectra labeled in Fig. 1 were recorded from different parts of the sample, since it had been etched between each measurement.

We will introduce two different definitions for the CLT's: one is caused by the onset of three-dimensional growth, denoted t_{3D}, and one is caused by the onset of dislocation formation, t_{dis}. The t_{3D}^P (the value of t_{3D} from the PL measurements) was indicated by a change in FWHM and a blueshift of the peak for increasing excitation density.[33,34] When the $In_{0.36}Ga_{0.64}As$ layer thickness reaches t_{dis}, the emission shifts to lower energy, broadens, and decreases in intensity.[3] The value of t_{dis} was not investigated in this work but from earlier published results[3,32] we can conclude that $t_{dis} > t_{3D}$.

For all examined samples with x between 0.36 and 1, the FWHM increased suddenly by a factor of 2 or more after reaching t_{3D}^P. This broadening was mainly caused by emission from excitons confined in wells with different thicknesses. In Fig. 2, t_{3D}^P is plotted as a function of growth temperature for different In content x. For $x=0.36$, t_{3D}^P exhibits a strong dependence on the growth temperature but as x increases the sensitivity to temperature becomes less pronounced. For $x=1$, the value of $t_{3D}^P=1$ ML, but a narrow FWHM could be achieved for 2-ML-thick QW's if the growth temperature was reduced below 490 °C.

B. RHEED measurements

At all growth temperatures, the RHEED pattern was characterized by streaks both for homoepitaxial and strained layer 2D growth. A change to a spotty pattern indicated a growth mode transition from 2D to 3D. For samples grown at 490 °C and below, the spotty pattern was suppressed and not as clear as for higher temperatures, which we interpret as due to a less pronounced island growth. In Fig. 3(a), the lattice parameter from RHEED measurements is shown as a function of layer thickness for the growth of $In_{0.36}Ga_{0.64}As$ at four different temperatures. Our previous extension of the CLT definition can also be applied here. The thickness at which 3D growth was first detected by RHEED occurred at the increases of lattice parameter and is denoted t_{c1}. Here the pattern also changed from a streaky to a spotty pattern. Exact determination of t_{dis} is difficult and occurs between t_{c1} and t_{c2}, the thickness where the lattice constant saturates. This is further discussed in Secs. IV C and IV D. As in the PL measurements, we found an increased CLT with decreasing growth temperature. Thus, t_{c2} varied from 10 to 95 Å between 590 °C and 490 °C, respectively. For high growth temperatures, t_{c2} was found to be close to the value of t_{c1}. As the growth temperature was reduced, the difference between t_{c1} and t_{c2} increased with a relatively higher value for t_{c2}. The solid curves in Fig. 3(a) are fitted calculations (from the DT model) to the experimental data. The calculation is further discussed in the Appendix.

Photos of the RHEED pattern in the [110] direction from the substrate, the GaAs buffer, and the strained layer 2D and 3D growth are shown in Figs. 3(c)–3(e). The (2×4) reconstruction (indicating an As-stabilized growth condition) improved during growth of the GaAs buffer. Growing the $In_{0.36}Ga_{0.64}As$ layer at 510–520 °C changed the reconstruction from (2×4) to (1×1). The streaky

pattern in Fig. 3(d) changed to the spotty pattern in Fig. 3(e) as the 3D growth was initiated.

C. Comparison between RHEED and PL data

Both PL and RHEED indicated a small variation of CLT with growth temperature above 530 °C but a large dependence below 520 °C. The complete change in the measured lattice parameter as observed by RHEED takes place between the two lower lines in Fig. 3(b). The most important result from Fig. 3(b) is the difference between the RHEED and PL data with relatively higher values for the PL measurements. Only t_{3D} was observed in the PL measurements but from previous TEM measurements[32] we have shown that 3D growth occurs prior to dislocation formation in embedded structures. Hence,

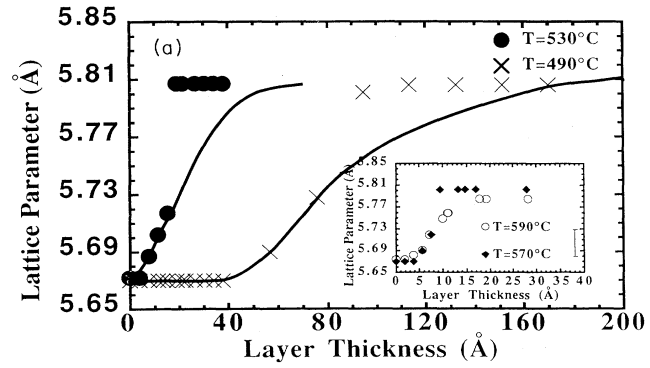

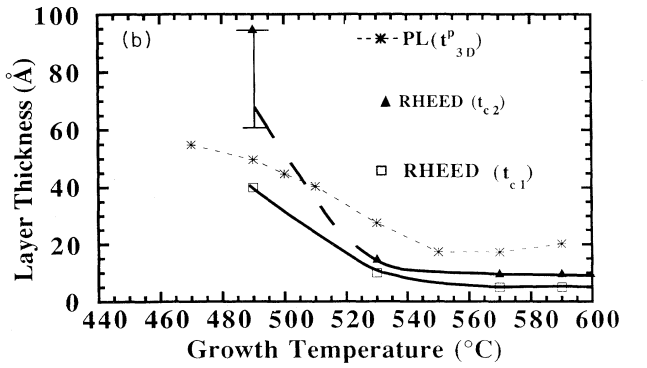

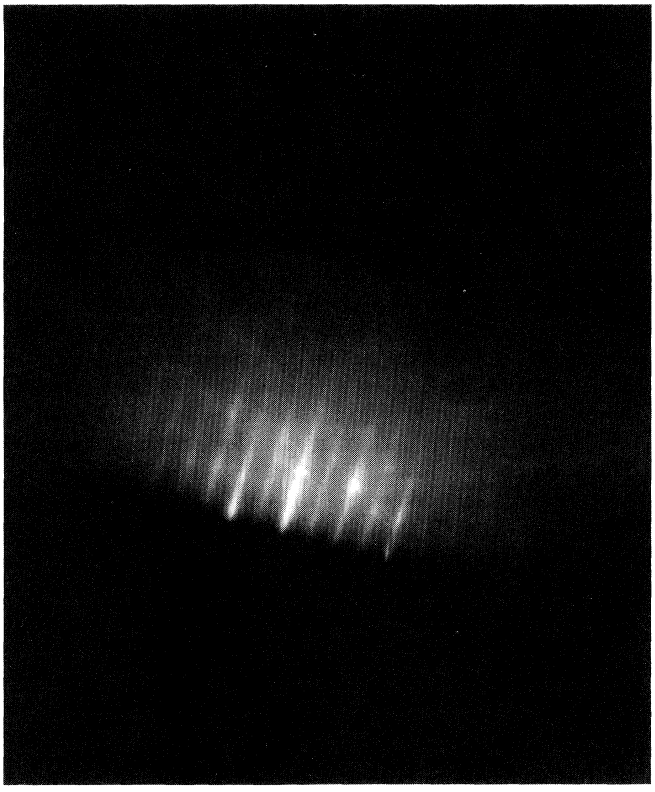

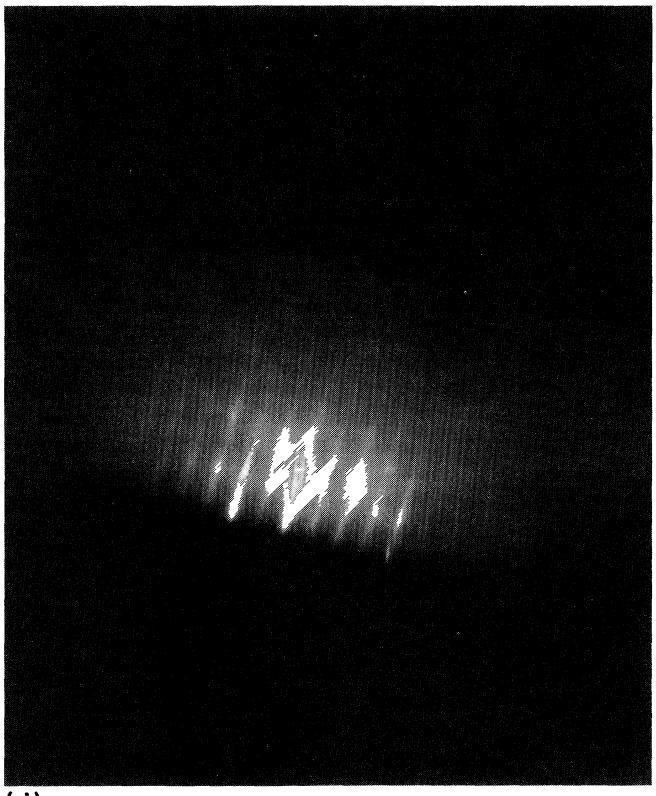

FIG. 3. (a) The lattice parameter for $In_{0.36}Ga_{0.64}As$ films as a function of layer thickness, measured *in situ* by RHEED for four different growth temperatures. The lines are calculated results. (b) A comparison between data from RHEED and PL measurements. The solid lines represent the RHEED measurement. The lower line t_{c1} shows the onset of 3D growth and the upper line is the fully relaxed lattice t_{c2}. The error bar on the upper RHEED data point, at 490 °C shows the uncertainty to determine when formation of dislocations starts. The broken line is t^{P}_{3D} from the PL measurements. (c) Photograph of the RHEED pattern after growth of 0.5-μm GaAs at 590 °C–600 °C. As the $In_{0.36}Ga_{0.64}As$ layer is deposited at 510 °C–520 °C the pattern changes as shown in (d) and (e). The 2D strained layer growth, shown by (d), is characterized by a streaky pattern. A spotty pattern appear as the growth mode switches from 2D to 3D.

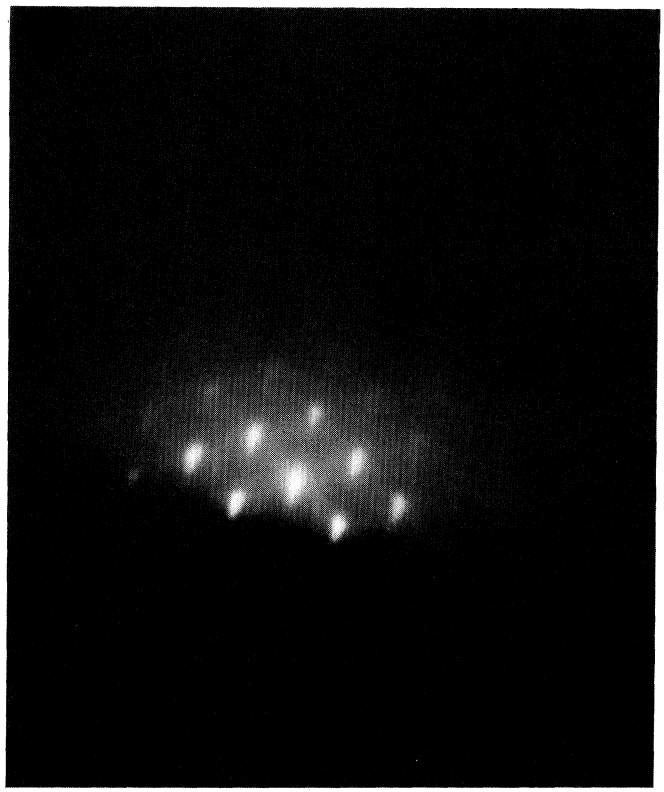

FIG. 3. (*Continued*).

both t_{3D} and t_{dis} are higher in the embedded PL structures than in the surface structures examined by RHEED. The resolution and detection limit for RHEED and PL are different and may influence the result. However, this difference is not large enough to explain the large discrepancy between the results from the two techniques. Instead, we attribute this to different dislocation formation mechanisms present in embedded as compared to surface layers.

D. Mobility measurements

The PL intensity was high but dropped quickly for all layers grown below 470 °C. Mobility measurements were made to find a possible correlation of this quenching of the luminescence to any electrical deterioration of the layers. A number of 2-μm-thick unintentionally doped n-type InAs layers were grown on GaAs at different temperatures. The carrier concentration showed only a small dependence, within a factor of 2, on growth temperature. Thus for a 300-K measurement, the carrier concentration varied only from 1.6 to 2.7×10^{16} cm^{-3} for layers grown at 525 °C and 410 °C, respectively, and between 9×10^{15} and 1.85×10^{16} cm^{-3} at 77 K. In Fig. 4(a) the carrier mobility μ_{300} is shown as a function of growth temperature. A 300 K a peak mobility of 17 266 cm^2/V s was measured in the layer grown under a diffuse (1×1) pattern at 520 °C. This has earlier been shown to be the optimum growth condition for InAs.[35] For growth below 520 °C, the mobility fell rapidly and was found to be ap-

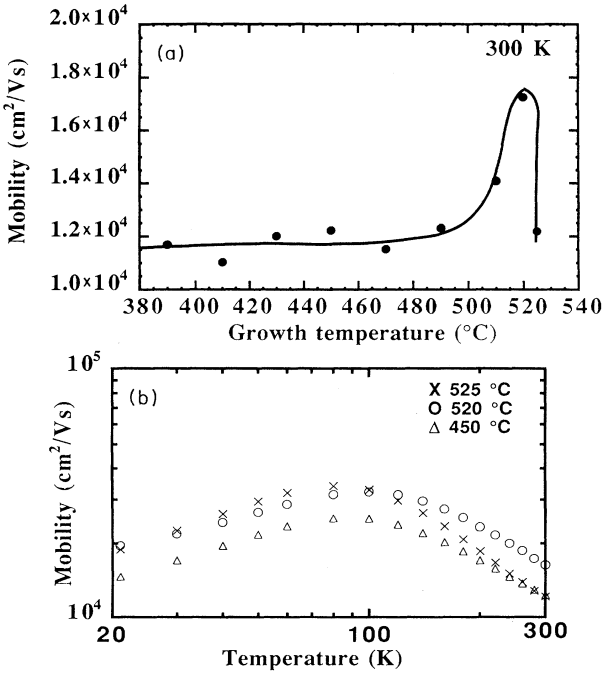

FIG. 4. (a) The Hall mobility at 300 K as a function of growth temperature. Growth temperatures below 510 °C had an increasing tendency to roughen the surface. The error bars shows the relative uncertainty in each measurement. (b) The mobility as a function of temperature for samples grown at three different temperatures.

proximately 12 000 $cm^2/V\,s$, independent of growth temperature. Also above 520 °C, with growth close to the (4×2) reconstruction, the mobility decreased. In Fig. 4(b) the mobility is shown as a function of temperature for three samples with growth temperature as a parameter. As can be seen, there is a peak mobility at approximately 80 K and the samples exhibit similar mobility curves. The sample grown at 520 °C had a mirrorlike surface with very few visible defects. Growth below 510 °C, or at 525 °C, gave rough surfaces as seen by optical microscopy. Clearly there is no obvious correlation between the mobility and the cutoff in PL intensity at 470 °C.

IV. DISCUSSION

A. Growth considerations

The surface ideally consists of atomic planar terraces separated by GaAs bilayer steps. The size of the terraces is of the order of 1000 Å, depending on the misorientation of the surface. In the 2D growth the impinging atoms move freely on the surface due to the high surface mobility. This growth can be separated into low- and high-temperature regimes.[36] At low temperatures the atomic surface migration distance is short and a 2D- nucleation occurs on the terraces. At high temperatures, where the mean free path of the surface atoms exceeds the terrace size, the atoms are preferably incorporated into lattice sites at the step edges. In the ideal 2D step growth mode, a local area of the exposed surface never consists of more than two unfinished monolayers. If there is a different lattice constant between surface layer and substrate, it is reasonable to assume that the growth mode switches from 2D to 3D at a critical strain. In this case, the impinging atoms form clusters (islands) on the surface and the growth front becomes rough. Both types of growth modes were detected by the RHEED pattern during growth. The 2D growth was characterized by streaks switching to a spotty pattern as 3D islands were nucleated on the surface. According to our PL data shown in Fig. 2, 3D islands are more rapidly formed at higher substrate temperature (with a low dependence on growth temperature when $x > 0.5$).

To explain these results, we suggest a simple schematic description. During growth there is a surface segregation of In atoms and a local segregation in the plane causing lateral inhomogeneities. The reduced temperature dependence with increased In content shown in Fig. 2 can be attributed to increased lateral segregation. This occurs since the edge atoms on these islands can attain a lattice parameter closer to that of the alloy before dislocations form (compare with Fig. 5). The impinging In atoms prefer to stick on top of growing islands since this is more energetically favorable than incorporation at the more strained lattice sites between the islands. During growth, the Ga atoms prefer incorporation in a less strained layer (the area between the nucleated islands), since this has a lattice parameter equal to GaAs. Such segregation will further increase the difference in lattice parameter between the islands and the fully strained layer. The variation of In content will thus cause a corresponding change in strain along the surface in addition to the vertical dependence. The driving force for this lateral segregation will increase as the difference in lattice mismatch between the strained layer and partly relaxed island increases. For a higher In content, this means that more In adatoms are incorporated in the islands. This causes a further strain reduction and the t_{3D} will decrease with increasing In content. A similar description of 3D growth has been given before.[37] It is difficult to estimate the degree of lateral segregation without access to high-resolution compositional analysis. The existence of surface segregation in the $In_xGa_{1-x}As/GaAs$ system has been shown before.[38–41] Recent work by Brandt *et al.*[28] attributes the surface segregation of In to strain-enhanced diffusion and other groups have observed a strain-reduced growth rate of highly strained material.

For high growth temperatures, $T \geq 560$ °C, the actual In content is reduced due to a decrease in the sticking coefficient. This was also observed in samples with $x = 0.36$, where t_{3D}^{P} increased for temperatures above 570 °C, see Fig. 2.

B. Photoluminescence

Photoluminescence spectra from quantum wells are largely related to interface morphology, which in turn is governed by the MBE-growth parameters. For thin QW's with $x = 0.36$–0.8, the PL emission was strong, with narrow FWHM, indicating smooth interfaces. However, the clear relation between measurement spot and the peak position and shape, as shown in Fig. 1, indicated a pseudosmooth interface.[42,43] The change from ideal 2D growth was initiated when the $In_xGa_{1-x}As$ growth front became incomplete and island thickness above one monolayer formed. When such average island sizes are smaller than the exciton Bohr radius, the energy position of the emission from the QW's will depend on the illumination spot and, consequently, the confinement potential for the exciton varies across the sample.[33,34]

As expected, the FWHM was independent of film thickness until it exceeded a certain value. Here, the peak intensity was still high but the FWHM suddenly increased by a factor of 2 to 3. Hence, a QW exhibiting this behavior does not contain misfit dislocations which reduces the PL intensity by several orders of magnitude and redshifts the peak energy. The sudden change can therefore be attributed to the onset of three-dimensional island formation.

As has been shown by TEM investigations,[32] 3D islands have a lateral size of approximately 250 Å, for a nominally 30-Å-thick $In_{0.36}Ga_{0.64}As$ layer. When the lateral size of the island exceeds the exciton Bohr radius (180 Å for $In_{0.5}Ga_{0.5}As$), at least two peaks can be resolved in the spectra. In Fig. 1 the emission at 1373.1 meV, curves (b) and (c), corresponds to excitonic recombination between carriers confined within islands and the peak at 1412.3 meV is from the "normal" QW areas between islands. At low excitation intensity the carriers occupy states within the islands since these have the lowest confinement energy. Increasing the laser intensity, these states saturate and the carriers occupy states in the

homogeneous layer. This part of the layer is thinner and therefore has a larger confinement energy than states related to island areas. The variation of the emission with excitation intensity is a typical feature after the onset of 3D growth. Earlier investigations also show that t_{3D} measured by TEM and PL exhibits a one-to-one correspondence.[44] For high excitation intensity and when the lateral island size is close to the exciton Bohr radius, emission originates from both islands and areas between them resulting in a very broad peak due to overlap from several peak energies.

C. Reflection high-energy electron diffraction

A change of lattice parameter will result in a corresponding change in spacing between the streaks in a RHEED pattern.[45] Hence, such a change indicates either a deformation of the lattice due to dislocation generation and multiplication or the onset of 3D growth. As shown in Fig. 3(a) there is a gradual change from the strained to the fully relaxed lattice. Earlier RHEED studies[15–17] revealed similar findings. A model for relaxation via plastic flow to describe this behavior was developed by Dodson and Tsao[21] (DT) for the Si_xGe_{1-x}/Si system. Based on calculations of the DT model, the activation energy for the dislocation glide for $In_{0.36}Ga_{0.64}As$/GaAs was estimated to be 3.9 eV which is larger than theoretical predictions[22,46] but close to earlier results.[16] As seen in Fig. 3(a) the fit between calculated and experimental results are poor. The calculation is described in detail in the Appendix. The high value for the activation energy for dislocation glide, the discrepancy between calculations and experimental results, and the number of fitting parameters indicates the limitations of the model to describe the detailed physical events when dislocations are formed.

We believe that the change in RHEED pattern is not only related to the formation of dislocations but also to the presence of strained islands and their shape as illustrated in Fig. 5. The edge atoms can adjust the lattice parameter close to that of the alloy without forming dislocations. After the 3D growth is nucleated, the material growing on top of the islands becomes less strained compared to a complete and strained layer. Due to surface segregation there are enough In atoms available for this. Thus, RHEED detects a change in lattice parameter before the structure relaxes since the electron diffraction is influenced in part by the lattice parameter of the islands. The thickness connected to dislocation formation, t_{dis}, cannot, therefore, be t_{c1}.

In addition, the extent of relaxation is connected to the layer thickness. Full relaxation of the lattice is not necessarily attained even after the formation of dislocations.[47–50] Determination of t_{dis} from RHEED measurements is therefore difficult and can only be restricted to the area between the lines t_{c1} and t_{c2} in Fig. 3(b).

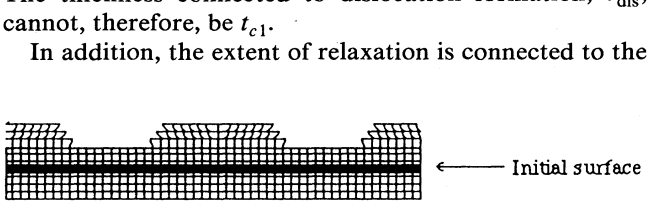

FIG. 5. A schematic illustration of the Stransky-Krastanov growth mode with strained islands. The edge atoms can attain a larger lattice parameter than that of GaAs without creation of dislocations. Both shape and symmetry have been exaggerated for the purpose of clarity.

D. Critical layer thickness

It is evident that lattice mismatched films grow in the Stransky-Krastanov mode. After initial condensation of 2D monolayers, there is an onset of 3D growth. This was detected by RHEED and corresponds to t_{c1} in Fig. 3(b). During single kink and half loop dislocation formation the lattice relaxes, which happens between lines t_{c1} and t_{c2} in Fig. 3(b). According to Matthews,[19] single kinks are formed from threading dislocations which glide at the interface. These single kinks are created when the misfit strain force exceeds the line tension force which acts to prevent the formation of misfit dislocations. However, because of the low initial density of threading dislocations present in the substrate material (10^4–10^5 cm^{-2}), it is not realistic that single kink formation is the only relaxation process. A second process comes from the creation of half loops at the growth front. When a half loop expands it forms a misfit dislocation line at the lower $In_xGa_{1-x}As$/GaAs interface and causes a relaxation of the lattice. If a GaAs cap is applied and the sum of the line tension forces is greater than the misfit strain force, the single kink will be pulled back resulting in coherent interfaces between the layers. On the other hand, if the misfit strain force in an embedded layer should exceed the line tension forces, a double kink will be formed. Under similar conditions, half loops can annihilate by the formation of paired dislocations, which is also described by MB.[18] Hence, the difference between CLT values measured by RHEED and by PL depends to a certain degree on the separate dislocation mechanisms present in surface and embedded layers. However, this does not explain when the PL measurement fails to indicate the initiation of the 3D growth which according to the RHEED measurements gives $t_{c1} < t_{3D}^P$. We believe that the islands created at t_{c1} are smaller than the Bohr radius of an exciton. As the island size increases with layer thickness, the GaAs/$In_xGa_{1-x}As$ interface adopts a wavelike shape giving rise to the t_{3D} measured by PL.

The RHEED measurement at 490 °C showed a higher CLT than PL, which we refer to difficulty to exactly judge when the lattice relaxation occurs. As can be seen in Fig. 3(a) the change is not as abrupt as for higher temperatures.

E. Calculation of the critical layer thickness

During the last two decades several models for the calculation of the critical layer thickness have been proposed. The following section describes and evaluates some of these. Models by Matthews[19] for surface layers. Matthews and Blakeslee[18] for embedded layers, Tsao and Dodson[21] (TD) and Price[51] consider a lack of force balance as responsible for the relaxation phenomenon. A

similar approach was adopted by People and Bean[20] but they considered an energy balance. In order to compare and establish under which conditions these models are valid, we have calculated t_{dis} from them. The results are presented in Fig. 6 and 7.

The model of Matthews describes dislocation mechanisms in a case where the misfit energy is shared between strain and dislocation generation. The different dislocation mechanisms were described in Sec. IV D. Mechanical equilibrium is maintained by two opposing forces, the line tension force and the strain force, expressed as

$$F_\varepsilon = \frac{2\mu(1+\nu)}{(1-\nu)} bh\varepsilon\cos\lambda \tag{1}$$

$$F_l = \frac{\mu b^2}{4\pi(1-\nu)}\left[(1-\nu\cos^2\alpha)\left[\ln\frac{h}{b}+1\right]\right] \tag{2}$$

where F_ε and F_l is the strain and line tension force, respectively, μ is the shear modules, b is the magnitude of the Burgers vector ($\approx$4 Å), ν is Poisson's ratio ($\approx$0.3), α and λ are different angles to describe the geometry of the dislocation and are set at 60°, ε is the value of strain, and h is the thickness of the strained layer. In a surface layer single kinks form when $F_\varepsilon > F_l$. An expression for the critical layer thickness can thus be formed by setting $F_\varepsilon = F_l$ which yields

$$h_c = \frac{b}{8\pi\varepsilon}\frac{(1-\nu\cos^2\alpha)}{(1+\nu)\cos\lambda}\left[\ln\frac{h_c}{b}+1\right]. \tag{3}$$

Similarly, a critical criterion for double kink formation

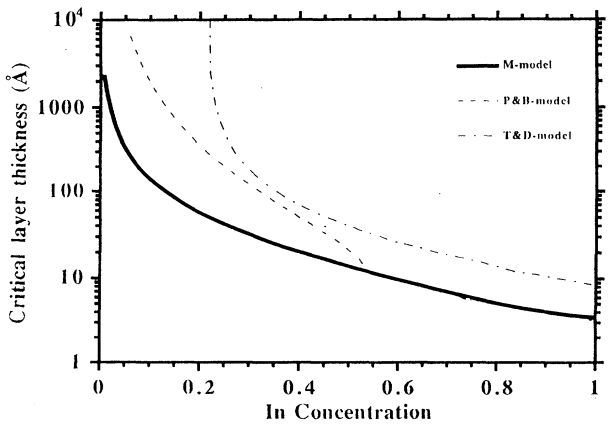

FIG. 6. The critical layer thickness as a function of In content calculated by three different models. Single kink dislocations are presumed in both the model of Matthews and the TD model. The curve representing the TD model is valid for structures grown at 490 °C where $\sigma_{exc}/\mu = 0.06$.

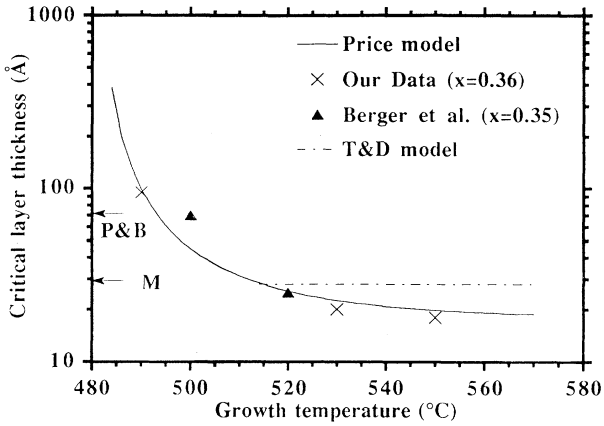

FIG. 7. The critical layer thickness as a function of growth temperature. The crosses and triangles represent our and Berger *et al.*'s (Ref. 17) experimental data, respectively. The solid line is a calculation from Price model assuming an activation energy for dislocation glide of 2.5 eV. The Tsao and Dodson model (dotted line) is temperature dependent up to 510 °C where $\sigma_{exc}/\mu = 0$ which corresponds to the value from the model by Matthews.

(MB model) in embedded structures is obtained by setting $F_\varepsilon = 2F_l$. The critical layer thickness for the single kink is shown in Figs. 6 and 7. We have, in an earlier paper[3] shown the ability of the MB models to agree with experimental results and become a guideline in the design of strained $In_xGa_{1-x}As/GaAs$ heterostructures. However, neither the model of Matthews nor the MB model depend on growth temperature, and as indicated in Fig. 7, they are valid only for structures grown at approximately 510 °C. In addition, the difference between the models and experimental results increases[52] for structures with a lattice mismatch below $\approx$2%.

For lower growth temperatures, both TD (Ref. 21) and Bean *et al.*[53] found larger t_{dis} than predicted by theory. Whaley and Cohen[15] showed that the lattice parameter for an $In_xGa_{1-x}As/GaAs$ heterostructure grown at 470 °C relaxed upon heating to the same values as for films grown at higher temperatures. An explanation of the phenomena was provided by Bean *et al.*,[53] who suggested the existence of a kinetic barrier at low growth temperatures, preventing dislocation formation and/or migration (metastable structures). To account for the metastablity, TD (Ref. 21) developed a model based on the MB model. According to TD the difference between the misfit strain and line-tension forces is the excess force. By normalizing this relation to the thickness of the strained layer an excess stress σ_{exc} was obtained. If σ_{exc} is below or equal to zero, the structure is stable, otherwise it is either metastable or relaxed. Hence, the excess stress may be defined as the driving force for relaxation of the lattice via dislocation generation. A more elaborate definition of the excess stress has been given in a recent paper by Freund and Hull.[54] The expression for the excess stress in a single kink (SK) dislocation is

$$\frac{\sigma_{\text{exc}}^{\text{SK}}}{\mu}(z)=\left|2\left\langle\frac{1+\nu}{1-\nu}\right\rangle\varepsilon\right|-\left\langle\frac{b^2}{4\pi}\right\rangle\left\langle\frac{1-\nu\cos^2\beta}{1-\nu}\right\rangle \times\frac{\ln\left\langle\frac{4h}{b}\right\rangle}{\frac{h}{b}} \tag{4}$$

with $\beta=60°$ assuming 60° mixed dislocations and the other symbols have their usual meaning. The factor 4 in the logarithm is an approximation and represents the core cutoff parameter that takes the core dislocation energy into account. Fitting this model to the experimental result from the structure grown at 490 °C reveals a value of σ_{exc}/μ of ≈ 0.06. In Fig. 6 the calculated t_{dis} using the TD model is shown assuming $\sigma_{\text{exc}}/\mu=0.06$. Note that this curve is valid only for surface layers grown at 490 °C. Trying to fit the model to structures grown above 510 °C gives negative values to the excess stress which is unphysical and indicates that the calculated t_{dis} is larger than the measured one. This may be a consequence of the influence of dislocations on surface and interfacial energies which will be important for thinner layers.[55] An error was also introduced in the model when the excess stress was obtained by normalizing the excess force with the thickness of the material above the interface assuming an atomically flat surface. Due to 3D growth, the thickness of the material above the interface varies from place to place, which causes the strain to depend on position (see Fig. 5). In Fig. 7 the curve representing the TD model is given only for temperatures above 510 °C by setting σ_{exc}/μ to zero which gives a value of the t_{dis} equivalent to the model by Matthews. The limitation of this model is clearly that no theoretical expression exists for σ_{exc}/μ. Hence, any temperature dependence can be obtained at least for temperatures below 510 °C. Limitations of this model have also been pointed out by Dirgo *et al.*[10]

A model which provides the best agreement with our experimental results was recently presented by Price.[51] Built on the work by Matthews and co-workers[19,56] it accounts both for the temperature and strain dependence of t_{dis} by introducing a "frictional force," F_f. This force represents the friction created when dislocations glide at the interface and is expressed by $F_t=Ah\exp(U/kT)$. The energy U is the activation energy for dislocation glide and is close to the Peierls energy, A is a constant and the other symbols have their usual meaning. Including forces for strain, line tension and surface step tension we have the following equation for mechanical equilibrium:

$$F_\varepsilon-F_l+F_s-F_f=0\ , \tag{5}$$

where F_ε and F_l are the strain and line-tension forces described in Eqs. (1) and (2). The term $F_s=\Gamma b\sin 60°$, which represents the tension in a surface step, becomes important when the layer thickness is below 50 Å. The surface energy represented by the factor Γ is of the order 1 J m^{-2} in analogy with the assumptions made in Price's paper. Good fits were obtained in the range $U=2.8\pm0.5$ eV and $\ln A=-51\pm9$. The curve in Fig. 7 is obtained with $U=2.5$ eV. It is in reasonable agreement with measurements of the activation energy for the dislocation glide in In-doped GaAs (Ref. 57) and better than the result obtained by the DT model (see the Appendix). A striking feature of the Price model is shown in Fig. 7 where t_{dis} rapidly increases towards infinity for growth temperatures below 490 °C. This has not been proven experimentally.

Generation of misfit dislocations have in the previously described models been determined by the mechanical equilibrium of existing threading dislocations and the nucleation of half loops. A different approach was adopted by People and Bean[20] who assumed that misfit dislocations are formed when the areal strain energy density exceeds the energy density connected to a screw dislocation. For $In_xGa_{1-x}As$ layers grown on GaAs we have

$$h_c=\frac{1.66\times10^{-2}}{\varepsilon^2}\ln\frac{h_c}{b} \tag{6}$$

with the usual meanings of the symbols. As indicated in Fig. 6 the model cannot predict t_{dis} for a strain higher than 4% and it lacks a temperature dependence.

F. Hall measurements

We expected that a large variation in growth temperature should change the incorporation of impurities and defects which in turn would influence the transport properties. The room-temperature electron mobility for thin InAs layers grown on GaAs is dominated by phonon and dislocation scattering.[58,59] As the measurement temperature is reduced the mobility becomes governed by ionized impurity and piezoelectric scattering. The transition occurred around 80 K where our InAs also showed the highest mobility, as seen in Fig. 4(b). However, the drastic reduction in mobility with decreased growth temperature, from 520 °C to 490 °C shown in Fig. 4(a), cannot be explained as a result of increased phonon and/or dislocation scattering. It has been shown that a critical relationship R_c exists between the As_4 and In partial pressures for a given growth temperature[60] ($R_c=p_{\text{As}_4}/p_{\text{In}}$). A deviation from the ideal R_c results in an As-rich or As-deficient growth front, with a subsequent reduction in mobility. All Hall samples, except the sample grown at 525 °C, were grown with the same As_2:In flux ratio. Samples grown at lower temperatures have a reduced mobility, since they were further away from the ideal As:In flux ratio (the surface was exposed to excess arsenic) than samples grown at higher substrate temperatures. It is also reasonable to assume a higher incorporation of impurities at low temperatures, which act to reduce the mobility further. The low 300 K mobility for the sample grown at 525 °C is taken as an indication of partial In nucleation (As deficiency), since this sample was grown in the vicinity of the (4×2) reconstruction.

V. CONCLUSION

We have demonstrated a relation between CLT and the growth temperature in a number of $In_xGa_{1-x}As/GaAs$

structures with x ranging from 0.36 to 1. The CLT, defined as the largest thickness of a strained, defect-free layer with sharp interfaces, was measured by RHEED and PL. Both techniques gave a similar trend; an increasing CLT with reduced growth temperature. A difference between the CLT values measured by PL and RHEED was explained in terms of different dislocation mechanisms acting in surface and embedded layers. Both phenomenological models and theoretical models were used to describe and predict t_{dis}. The best fit to our experimental results was obtained using the recently proposed model by Price.[51] The mobility was found to decrease with reduced growth temperature, which was attributed to increasing concentrations of impurities and defects.

ACKNOWLEDGMENTS

Pong Songpongs is acknowledged for the Hall-effect measurements, Anders Carlström for use of the Teragon system, and P. I. Cohen and A. M. Dabiran for private communication. The Swedish National Board for Industrial and Technical Development (NUTEK) is acknowledged for financial support.

APPENDIX: TIME-DEPENDENT RELAXATION OF STRAINED STRUCTURES

Based on a model by Alexander and Haasen,[46] further developed by Dodson and Tsao[21] (DT), results from the RHEED measurements were used to predict t_{dis} and also to calculate an activation energy for dislocation glide. Such an approach was earlier adopted by Whaley and Cohen[16] and revealed an activation energy of 4.4 eV for $In_{0.33}Ga_{0.67}As/GaAs$ heterostructures.

In the DT model the time-dependent strain relaxation is described with a differential equation

$$\frac{\partial\gamma(t)}{\partial t}=C[f_0-\gamma(t)-r(h)]^2[\gamma(t)+\gamma_0]\ , \tag{A1}$$

where

$$\gamma(t)=\frac{[a(t)-a_0]}{a_0}\ . \tag{A2}$$

Here, $a(t)$ is the relaxed and a_0 the unrelaxed lattice parameter, γ_0 represents a background source for dislocations, and C is the relaxation coefficient. The relative difference in lattice parameter between substrate and unstrained layer is expressed by $f_0=r(h_c)$ where h_c is the critical thickness according to MB,[18,19] and $r(h)$ is the residual strain at equilibrium

$$r(h)=\frac{1}{4\pi}\frac{1-\nu\cos^2\beta}{1+\nu}\frac{\ln\left[\frac{4h}{b}\right]}{\frac{h}{b}}\ , \tag{A3}$$

where b is the magnitude of the Burgers vector (slip distance), ν is Poisson's ratio ($\nu\approx 0.3$), h is the thickness of the strained layer, and β defines the dislocation orientation. The present model incorporates two variables which each can be adjusted to obtain a fit to the experimental data. Varying γ_0 gave only small changes and was fixed to 3×10^{-5}. A variation of the only remaining variable, the relaxation coefficient C, did not enable a fit to the experimental data. We found that the model could describe the experimental results best by setting $r(h)$ to 50% of the result from Eq. (A3).

Assuming that the model is correct this implies either an incapability of RHEED to see the early stages of relaxation or that the expression for the residual strain at equilibrium is not correct. We have not been able to find any support in the literature for such limitations of RHEED. The latter implication concerning limitations in the expression for the residual strain is supported in a paper by Dirgo *et al.*[10] However, their experimental findings do not support the DT model.

The solid curves in Fig. 3(b) were calculated to fit the experiment for different growth temperatures assuming that $\delta\gamma(t)/\delta t=\delta\gamma(h)/\delta h * R$, where R is the growth rate. It was not possible to obtain a good agreement for the layers grown at 570 °C and 590 °C without a further reduction of the $r(h)$ factor, below 50%. As can be seen from Fig. 3 the fit was best at the beginning of the relaxation process. A better fit close to the commencement of the totally relaxed part of the curve could be made at the expense of the good fit at the onset of relaxation. In this case it was obtained much earlier than the experiment showed and was therefore avoided.

A number of different C parameters were obtained by fitting the model to experimental results. The activation energy for the dislocation glide U could be extracted since $C\sim\exp(-U/kT)$. This gave $U\approx 3.9$ eV. This is lower than the 4.4 eV calculated by Whaley and Cohen[16] but still above theoretical estimations[22,46] and other experimental results.[51,57]

[1] I. J. Fritz, S. T. Picraux, L. R. Dawson, and T. J. Drummond, Appl. Phys. Lett. **46**, 967 (1985).
[2] N. G. Anderson, W. D. Laidig, R. M. Kolbas, and Y. C. Lo, J. Appl. Phys. **60**, 2361 (1986).
[3] T. G. Andersson, Z. G. Chen, V. D. Kulakovskii, A. Uddin, and J. T. Vallin, Appl. Phys. Lett. **51**, 752 (1987).
[4] I. J. Fritz, P. L. Gourley, and L. R. Dawson, Appl. Phys. Lett. **51**, 1004 (1987).
[5] P. L. Gourley, I. J. Fritz, and L. R. Dawson, Appl. Phys. Lett. **52**, 377 (1988).
[6] J.-P. Reithmeier, H. Cerva, and R. Lösch, Appl. Phys. Lett. **54**, 48 (1989).
[7] S. L. Weng, J. Appl. Phys. **66**, 2217 (1989).
[8] P. J. Orders and B. I. Usher, Appl. Phys. Lett. **50**, 980 (1987).
[9] C. W. Wie, J. Appl. Phys. **65**, 2267 (1989).
[10] A. V. Dirgo, A. Aydinli, A. Carnera, F. Genova, C. Rigo, C. Ferrari, P. Franzosi, and G. Salviati, J. Appl. Phys. **66**, 1975 (1989).
[11] P. M. J. Marée, J. C. Barbour, J. F. Van der Veen, K. L. Kavanagh, C. W. T. Bulle-Lieuwma, and M. P. A. Viegers, J.

Appl. Phys. **62**, 4413 (1987).
[12]A. Fischer-Colbrie, J. N. Miller, S. S. Laderman, S. J. Rosner, and R. Hull, J. Vac. Sci. Technol. B **6**, 620 (1988).
[13]G. L. Price, Appl. Phys. Lett. **53**, 1288 (1988).
[14]B. Elman, E. S. Kotelas, P. Melman, C. Jagannath, Johnson Lee, and D. Dugger, Appl. Phys. Lett. **55**, 1659 (1989).
[15]G. J. Whaley and P. I. Cohen, J. Vac. Sci. Technol. B **6**, 625 (1988).
[16]G. J. Whaley and P. I. Cohen, Appl. Phys. Lett. **57**, 144 (1990).
[17]Paul R. Berger, Kevin Chang, Pallab Bhattacharya, and Jasprit Singh, Appl. Phys. Lett. **53**, 684 (1988).
[18]J. W. Matthews and A. E. Blakeslee, J. Cryst. Growth **27**, 118 (1974).
[19]J. W. Matthews, J. Vac. Sci. Technol. **12**, 126 (1975).
[20]R. People and J. C. Bean, Appl. Phys. Lett. **47**, 322 (1985); **49**, 229 (1986).
[21]J. Y. Tsao and B. W. Dodson, Appl. Phys. Lett. **53**, 848 (1988).
[22]B. W. Dodson and J. Y. Tsao, Appl. Phys. Lett. **51**, 1325 (1987); **52**, 852 (1988).
[23]B. W. Dodson and J. Y. Tsao, Phys. Rev. B **38**, 12 383 (1988).
[24]J. Zang, E. M. Gibson, C. T. Foxon, and B. A. Joyce, J. Cryst. Growth **111**, 93 (1991).
[25]K. Woodbridge, K. J. Moore, N. L. Andrew, and P. F. Fewster, J. Cryst. Growth **111**, 339 (1991).
[26]M. T. Emeny, L. K. Howard, K. P. Homewood, and J. D. Lambkin, J. Cryst. Growth **111**, 413 (1991)
[27]J. P. Reithmaier, H. Riechert, H. Schlötterer, and G. Weimann, J. Cryst. Growth, **111**, 407 (1991).
[28]O. Brandt, L. Tapfer, K. Ploog, M. Hohenstein, and F. Phillipp, J. Cryst. Growth **111**, 383 (1991).
[29]O. Brandt, L. Tapfer, R. Cingolani, M. Ploog, M. Hohenstein, and F. Phillipp, Phys. Rev. B **41**, 12 599 (1990).
[30]M. J. Ekenstedt, T. G. Andersson, and H. Millqvist, in *Proceedings of the 14th Nordic Semiconductor Meeting,* edited by O. Hansen (Institute of Physics, University of Århus, Århus, Denmark, 1990), p. 47.
[31]M. J. Ekenstedt and T. G. Andersson, J. Vac. Sci. Technol. B **9**, 1605 (1991).
[32]J. Y. Yao, T. G. Andersson, and L. Dunlop, Appl. Phys. Lett. **53**, 1420 (1988).
[33]M. J. Ekenstedt, S. M. Wang, and T. G. Andersson, Appl. Phys. Lett. **58**, 854 (1991).
[34]S. M. Wang, T. G. Andersson, and M. J. Ekenstedt, Appl. Phys. Lett. **59**, 2156 (1991).
[35]S. M. Newstead, R. A. A. Kubiak, and E. H. C. Parker, J. Cryst. Growth **81**, 49 (1987).
[36]J. H. Neave, P. J. Dobson, B. A. Joyce, and J. Zhang, Appl. Phys. Lett. **47**, 100 (1985).
[37]C. W. Snyder, B. G. Orr, D. Kessler, and L. M. Sander, Phys. Rev. Lett. **66**, 3032 (1991).
[38]C. Guille, F. Houzay, J. M. Moison, and F. Barthe, Surf. Sci. **189/190**, 1041 (1987).
[39]J. M. Moison, C. Guille, F. Houzay, F. Barthe, and M. Van Rompay, Phys. Rev. B **40**, 6149 (1989).
[40]J-M. Gerard and J-Y. Marzin, Phys. Rev. B **45**, 6313 (1992).
[41]K. Muraki, S. Fukatsu, and Y. Shiraki, Appl. Phys. Lett. **61**, 557 (1992).
[42]S. Munnix, R. K. Bauer, D. Bimberg, J. S. Harris, Jr., R. Köhrbrück, E. C. Larkins, Ch. Maierhofer, D. E. Mars, and J. N. Miller, J. Vac. Sci. Technol. B **7**, 704 (1989).
[43]R. F. Kopf, E. F. Schubert, T. D. Harris, and R. S. Becker, Appl. Phys. Lett. **58**, 631 (1991).
[44]S. M. Wang, T. G. Andersson, V. D. Kulakovskii, and J. Y. Yao, Superlatt. Microstruct. **9**, 123 (1991).
[45]I. Hernández-Calderón and H. Höchst, Phys. Rev. B **27**, 4961 (1983).
[46]H. Alexander and P. Haasen, Solid State Phys. **22**, 27 (1968).
[47]F. C. Frank and J. V. van der Merwe, Proc. R. Soc. London, Ser. A **189**, 205 (1949).
[48]C. A. B. Ball and J. H. van der Merwe, Phys. Status Solidi **38**, 335 (1970).
[49]C. A. B. Ball, Phys. Status Solidi **42**, 357 (1970).
[50]Ji-Yong Yao and T. G. Andersson, J. Appl. Phys. **69**, 2224 (1991).
[51]G. L. Price, Phys. Rev. Lett. **66**, 469 (1991).
[52]B. Elman, Emil S. Koteles, P. Melman, K. Ostreicher, and C. Sung, J. Appl. Phys. **70**, 2634 (1991).
[53]J. C. Bean, L. C. Feldman, A. T. Fiory, S. Nakahara, and I. K. Robinson, J. Vac. Sci. Technol. A **2**, 436 (1984).
[54]L. B. Freund and R. Hull, J. Appl. Phys. **71**, 2054 (1992).
[55]B. W. Dodson and I. J. Fritz, Cryst. Prop. Prep. **21**, 29 (1989).
[56]J. W. Matthews, S. Mader, and T. B. Light, J. Appl. Phys. **41**, 3800 (1970).
[57]N. Burle-Durbec, B. Pichaud, and F. Minari, Philos. Mag. Lett. **56**, 173 (1987).
[58]S. Kalem, J-I. Inn Chyi, H. Morkoc, R. Bean, and Ken Zanio, Appl. Phys. Lett. **53**, 1647 (1988).
[59]M. J. Ekenstedt, P. Songpongs, and T. G. Andersson, Appl. Phys. Lett. **61**, 789 (1992).
[60]R. A. A. Kubiak, E. H. C. Parker, and S. Newstead, Appl. Phys. A **35**, 61 (1984).

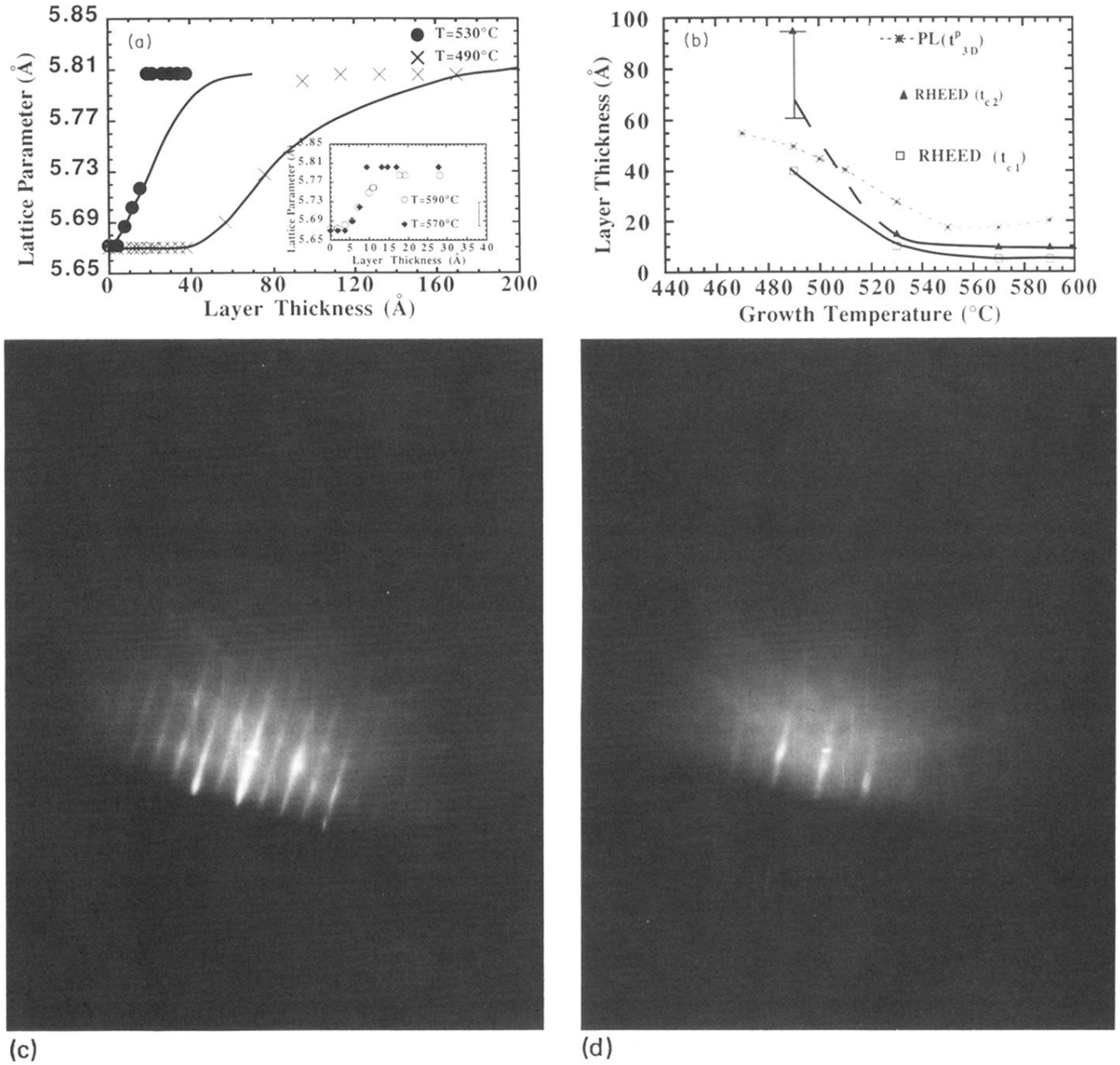

FIG. 3. (a) The lattice parameter for $In_{0.36}Ga_{0.64}As$ films as a function of layer thickness, measured *in situ* by RHEED for four different growth temperatures. The lines are calculated results. (b) A comparison between data from RHEED and PL measurements. The solid lines represent the RHEED measurement. The lower line t_{c1} shows the onset of 3D growth and the upper line is the fully relaxed lattice t_{c2}. The error bar on the upper RHEED data point, at 490 °C shows the uncertainty to determine when formation of dislocations starts. The broken line is t^P_{3D} from the PL measurements. (c) Photograph of the RHEED pattern after growth of 0.5-μm GaAs at 590 °C–600 °C. As the $In_{0.36}Ga_{0.64}As$ layer is deposited at 510 °C–520 °C the pattern changes as shown in (d) and (e). The 2D strained layer growth, shown by (d), is characterized by a streaky pattern. A spotty pattern appear as the growth mode switches from 2D to 3D.

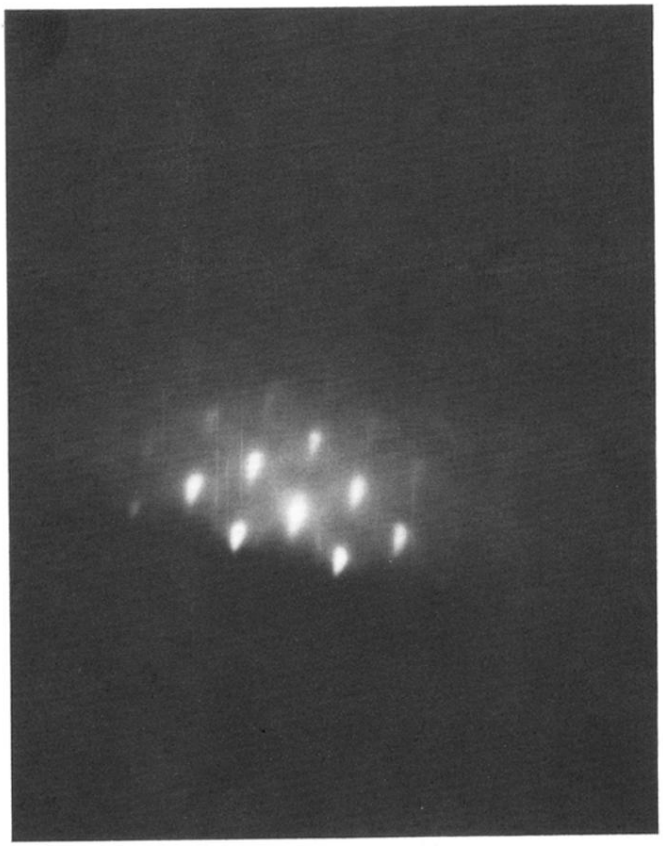

(e)

FIG. 3. (*Continued*).